

Ichnaea: A Low-overhead Robust WLAN Device-free Passive Localization System

Ahmed Saeed, *Student Member, IEEE*, Ahmed E. Kosba, *Student Member, IEEE*, and Moustafa Youssef, *Senior Member, IEEE*

Abstract—WLAN Device-free passive (*DfP*) indoor localization is an emerging technology enabling the localization of entities that do not carry any devices nor participate actively in the localization process using the already installed wireless infrastructure. Current state-of-the-art *DfP* localization systems require a large overhead to construct an RF profile for the environment, that is then used as a reference for either motion detection or tracking. These profiles are also not robust to changes in the environment, requiring frequent manual maintenance or reconstruction.

In this paper, we present the design, implementation and evaluation of *Ichnaea*, an accurate, robust, and low-overhead *DfP* localization system. *Ichnaea* uses a lightweight, typically two minutes, training period to learn the silence profile of the environment. It then applies statistical anomaly detection techniques and particle filtering, while adapting to changes in the environment, to provide its localization capabilities using standard WiFi hardware. Evaluation of *Ichnaea* in three typical testbeds with a side-by-side comparison to the state-of-the-art WLAN *DfP* systems shows that it can achieve a worst case median distance error of 2.5m while requiring significantly lower deployment overhead and being robust to environment changes.

Index Terms—Anomaly detection, device-free passive localization, particle filters, robust device-free localization.

I. INTRODUCTION

THE increasing need for context-awareness in modern consumer applications and the rapid advancements in communication networks have motivated significant research effort in the area of location-based services. This effort resulted in the development of many location determination systems, including the GPS system [7], ultrasonic-based systems [24], infrared-based (IR) systems [33], and radio frequency-based (RF) systems [37]. These systems require the tracked entity to carry a device that participates in the localization process. Thus, we refer to them as device-based systems.

Recently, the idea of RF device-free localization, where an entity can be tracked without any devices attached to it nor participating actively in the localization process, has been introduced [13], [19], [28], [29], [34], [36]. Based on RF signal processing, these systems have an advantage over traditional device-free tracking systems such as cameras [14] and IR-based systems as these later systems are limited to line-of-sight vision and thus the cost of covering an area

might be prohibitive. In addition, regular cameras fail to work in the dark or in the presence of smoke. Applications of RF-based device-free localization include intrusion detection, border protection, patient monitoring, and smart homes.

A special class of RF device-free localization systems is those based on standard wireless networks. In particular, the work in [36] introduced a device-free passive (*DfP*) localization system that works with standard wireless LANs. The basic idea depends on the fact that the presence and motion of entities in an RF environment affect the RF signal strength especially when dealing with the 2.4 GHz band which is used in different IEEE standards such as 802.11b and 802.11g (WiFi). This class of device-free localization systems is particularly challenging as it requires relying on a small number of sensory nodes (i.e. WiFi access points and receivers). Moreover, the deployment of such systems is usually within indoor areas rich in multipath, which makes tracking the effect of human presence on RSS values challenging.

A typical *DfP* system consists of signal transmitters, such as access points (APs), signal receivers or monitoring points (MPs), such as standard laptops, and an application server which collects and processes information about the received signals from each MP. The application server contains the main system modules responsible for performing its different localization functions. Several WLAN *DfP* algorithms were proposed for human motion detection [19], [36] and tracking [13], [28], [29], [35], [36] of entities in indoor environments. These *DfP* systems provide a software only solution on top of the already installed wireless networks and hence provide a value-added service to these networks without adding any special hardware.

Current WLAN *DfP* localization techniques [19], [28], [29], [35], [36] provide good performance under strong operation assumptions, which limit their application domain. For example, the techniques proposed in [19], [28], [29], [35] require the construction of human presence profiles in the form of either human motion profiles [19] or passive radio maps [28], [29], [35]. These profiles lead to a high calibration overhead for large-scale environment deployments. In addition, access to the entire area of interest is required and professionals are needed to perform this calibration which might require access to restricted or private areas. Moreover, these systems are not robust to changes in the environment which affects their accuracy as changes to the environment, e.g. humidity and temperature changes, occur. This requires either frequent manual maintenance or even worse, reconstruction of the high-overhead human presence profiles.

A. Kosba is with the Department Computer Science, University of Maryland, College Park, USA. E-mail: akosba@cs.umd.edu

A. Saeed and M. Youssef are with the Department of Computer Science and Engineering Egypt-Japan University of Science and Technology and Alexandria University. E-mail: {ahmed.saeed, moustafa.youssef}@ejust.edu.eg

*An earlier version of this paper appeared in Percom 2012 [12].

In this paper, we present *Ichnaea*: a novel WLAN *DfP* localization system with the goals of providing low-overhead, accurate, and robust motion detection and tracking capabilities. *Ichnaea* performs its functionalities in three steps: First, it constructs an initial non-parametric **silence** profile for the signal strength readings received at the MPs. This step is performed to capture the behavior of the received signal strength at the different MPs when no humans are present in the area of interest during a short training period (typically two minutes for the whole area). Second, *Ichnaea* uses statistical anomaly detection techniques to detect streams exhibiting anomalous behavior due to the effect human presence has on the streams. Concurrently, *Ichnaea* also employs techniques for continuously updating its silence profile to adapt to the environment changes ensuring the system robustness. Third, the anomaly scores assigned to each wireless stream are then used by a *particle filtering algorithm* to track the exact motion path of the moving entity. Currently, we focus on enabling tracking of a single entity leaving the multi-entity tracking problem to a future paper.

We evaluate *Ichnaea* in three large-scale typical testbeds rich in multi-path and compare its performance to the state-of-the-art WLAN *DfP* detection and tracking techniques [19], [28], [35], [36]. Our results show that *Ichnaea* achieves its goals of high accuracy, low-overhead and robustness.

In summary, the contributions of this paper are three-fold:

- We present the design of *Ichnaea*, a low-overhead robust WLAN *DfP* localization system that employs statistical anomaly detection and particle filtering to detect and track human motion using conventional WLAN deployments.
- We present techniques that allow *Ichnaea* to adapt to environment changes and reduce the effect of the wireless channel noise.
- We evaluate the system in three large-scale realistic testbeds and compare it to the state-of-the-art *DfP* detection and tracking techniques.

The rest of the paper is organized as follows: Section II gives the details of the system while Section III shows its performance evaluation. In Section IV we compare *Ichnaea* to the state-of-the-art WLAN *DfP* detection and tracking techniques. Section V discusses related work. We finally conclude the paper in Section VI.

II. THE ICHNAEA SYSTEM

In this section, we give the details of the *Ichnaea* system. We start by an overview of the system architecture followed by the details of the system modules.

A. System Overview

Figure 1 shows the system architecture. The modules of the proposed system are implemented in the application server that collects samples from the monitoring points and processes them. The system works in two phases:

- 1) A short *offline* phase, during which the system studies the signal strength values when no human is present inside the area of interest to construct what we call

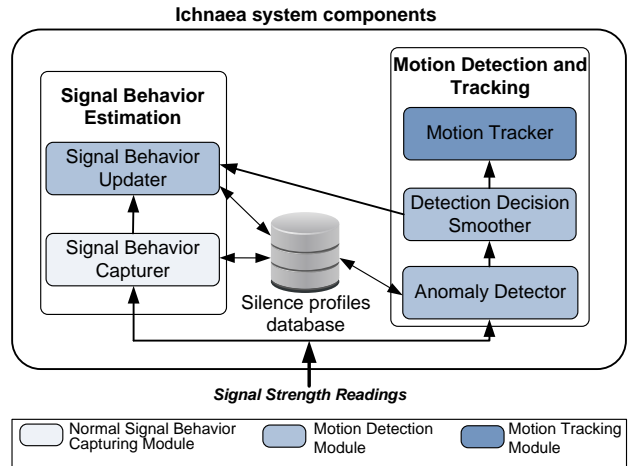


Fig. 1. *Ichnaea* system architecture.

a “**normal or silence profile**” for each stream. The profiles of all streams are constructed concurrently in that short phase.

- 2) A *monitoring* phase, in which the system collects readings from the monitoring points and decides whether there is human activity (anomalous behavior) or not based on the information gathered in the offline phase. Based on the detected anomalous streams, a particle filtering algorithm is used to track the motion through the area of interest. Moreover, the stored normal profile are also updated to adapt to environment changes.

The *Normal Signal Behavior Capturing Module* captures the behavior of the signal streams when there is no human motion present in the area of interest and stores initial silence profiles based on a short training period (Section II-C).

The *Anomaly Detector Module* examines each stream readings in the monitoring phase and decides whether they exhibit anomalous behavior or not. This operation is applied to each stream independently. It also assigns an anomaly score to each stream to express the intensity of the anomalous behavior (Section II-D1).

The *Detection Decision Smoother Module* fuses the anomaly scores of the different streams to reduce the noise and enhance the overall detection accuracy (Section II-D2).

The *Signal Behavior Updater Module* continuously updates the normal profiles constructed in the offline phase in order to adapt to changes in the environment (Section II-D3).

The *Motion Tracking Module* works after a motion detection alarm has been raised. It uses the anomaly score assigned to each stream to give weights to different particles representing the possible tracked entity location. Combined with a human motion model, these weights are used by a particle filter to infer the current location of the moving entity (Section II-E).

For the balance of this section, we start by giving the mathematical notations followed by the details of the different modules.

B. Mathematical Notations

Table I summarizes the symbols used. Let k be the number of streams, which is equal to the number of APs times

Symbol	Description
k	Number of streams
S_t	Received signal strength vector at time instant t
$s_{j,t}$	Received signal strength for stream j at time instant t
$\tilde{W}_{j,t}$	Sliding window of received signal strength values for stream j at time instant t
l	Size of received signal strength sliding window ($ \tilde{W}_{j,t} $)
$g(\cdot)$	Feature mapping function
$x_{j,t}$	Feature value for sliding window $\tilde{W}_{j,t}$
$a_{j,t}$	Anomaly score for sliding window $\tilde{W}_{j,t}$
a_t	Global anomaly score at time instance t
B_t	Smoothed value of the global anomaly score at time instance t
α	Significance
l_{update}	Number of consecutive $x_{j,t}$ forming an update window
r_t	Coordinates of the tracked moving entity at time t
$r_{i,t}$	Particle i representing a possible value for r_t
$z_{j,t}$	Weight assigned to particle i based on the anomaly score of stream j at time t
$z_{i,t}$	Overall particle i weight at time t
d_j	Length of stream j (distance between the AP and MP of the stream)
$d_{\text{AP},i}$	Distance between particle i and the AP of stream j
$d_{\text{MP},i}$	Distance between particle i and the MP of stream j

TABLE I
LIST OF SYMBOLS USED.

the number of MPs. Let $S_t = \{s_{j,t} | j = 1, \dots, k\}$ denote the received signal strength (RSS) readings vector at time t composed of k readings, one for each stream j . The system studies the behavior of a sliding window $W_{j,t}$ of size l that ends at time t , i.e. $W_{j,t} = [s_{j,t-l+1}, s_{j,t-l+2}, \dots, s_{j,t}]$.

In order to study the behavior of the sliding windows, each sliding window $W_{j,t}$ is mapped to a single *feature* or value $x_{j,t}$ through a function $g(\cdot)$. For example, if the mean is the selected feature, then $g(W_{j,t}) = \frac{1}{l} \sum_{i=1}^l s_{j,t-l+i}$. Our experiments show that measures of dispersion or variation, such as the variance, are superior signal features in terms of robustness to profile changes and sensitivity to human activity [12]. Thus, for the rest of the paper, we use the sample variance as the selected feature. It should be noted that using the full sliding window vectors for anomaly detection, without mapping it to a single feature, leads to increased complexity, which reduces the responsiveness of the system.

C. Normal Signal Behavior Capturing Module

The purpose of the *Normal Signal Behavior Capturing Module* is to construct a silence profile for each stream, capturing the received signal strength characteristics when there is no human in the area of interest. This is used later by other modules to detect anomalies in signal strength readings caused by human presence. This module runs in the offline phase. It extracts the feature values from the sliding windows over the collected data and estimates its distribution. We experimented with a number of density estimation techniques and found that using non-parametric kernel density estimation provides good results with reasonable complexity [13]. This operation is performed for each stream independently (Figure 2).

Formally, for a stream j , given a set of n sliding windows, each of length l samples, i.e. there are $n + l - 1$ readings collected, each window $W_{j,i}$ is mapped to a value $x_{j,i}$, where $x_{j,i} = g(W_{j,i})$. Assume f_j is the density function representing the distribution of the observed $x_{j,i}$'s, then given a random

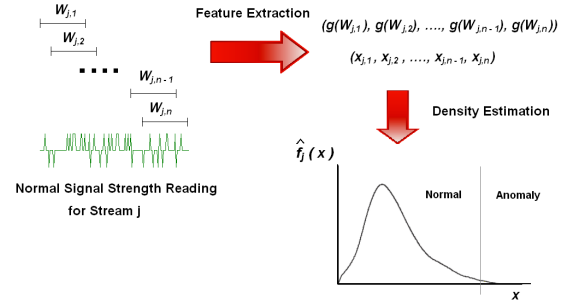


Fig. 2. Illustration of the normal profile construction.

sample $x_{j,1}, x_{j,2}, \dots, x_{j,n}$, the estimated density function \hat{f}_j is given by [30]:

$$\hat{f}_j(x) = \frac{1}{nh_j} \sum_{i=1}^n V\left(\frac{x - x_{j,i}}{h_j}\right) \quad (1)$$

where h_j is the bandwidth and V is the kernel function. The choice of the kernel function is not significant for the results of the approximation [27]. Hence, we choose the Epanechnikov kernel as it is bounded and efficient to integrate:

$$V(q) = \begin{cases} \frac{3}{4}(1 - q^2), & \text{if } |q| \leq 1 \\ 0, & \text{otherwise} \end{cases} \quad (2)$$

Also, we used Scott's rule to estimate the optimal bandwidth [27]:

$$h_j^* = 2.345\hat{\sigma}_j n^{-0.2} \quad (3)$$

where $\hat{\sigma}_j$ is an estimate for the standard deviation for the $x_{j,i}$'s.

After estimating the density function for the variance extracted from the sliding windows, a critical upper bound for the variance is calculated so that if the variance observed in the monitoring state exceeds this bound, the observed values are considered anomalous. In particular, given a significance parameter α and assuming \hat{F}_j is the CDF of distribution shown in Equation 1, then the bound is equal to $\hat{F}_j^{-1}(1 - \alpha)$.

D. Motion Detection Module

The *Motion Detection Module* runs during the monitoring phase to detect human presence in the area of interest. It has three functionalities: (1) to detect signal strength anomalies, i.e. human presence, based on the signal profiles constructed during the offline phase (2) to take a collective decision based on the anomalies detected for individual streams to decide whether a human was detected or not, and (3) to update the stored signal profiles to adapt to changes in the environment.

This decision is then used to trigger the *Motion Tracking Module*. For the rest of this section, we present the details of the three functionalities of this module.

1) *Anomaly Detector*: This procedure is responsible for detecting anomalous behavior exhibited by any of the streams based on the collected silence profiles. In particular, for a window of samples $W_{j,t}$ for stream j at a given time instant t , the module calculates the corresponding feature value $x_{j,t}$, i.e. the sample variance. A stream j is considered anomalous

if $x_{j,t}$ is above a critical bound u_j . Given a significance parameter α and assuming \hat{F}_j is the CDF of distribution shown in Equation 1, the upper bound u_j is equal to the $100(1-\alpha)^{th}$ percentile of the CDF function, such that

$$u_j = \hat{F}_j^{-1}(1-\alpha) \quad (4)$$

The module calculates an anomaly score $a_{j,t}$ for each stream j to keep track of the significance of any anomalous activity as:

$$a_{j,t} = \frac{x_{j,t}}{u_j}, \text{ where } \begin{cases} a_{j,t} < 1 & \text{if no anomaly is detected} \\ a_{j,t} \geq 1 & \text{if anomaly is detected} \end{cases} \quad (5)$$

where $x_{j,t}$ is the sample variance of the window and u_j is the critical value. This initial procedure requires two parameters: the window size l and the significance α . Analysis of the effect of both parameters on performance is presented in Section III-C. We finally note that processing each stream individually helps with tracking and visualization and reduces the complexity of updating the silence profile distributions.

2) *Detection Decision Smoother*: Typical wireless environments are noisy. This fact can cause many false alarms if we declare a detection event based on the result of any single stream alone. This could also degrade the performance of motion tracking significantly by starting the tracking procedure unnecessarily. To avoid this degradation, this sub-module studies the behavior of a global state of all streams.

The global anomaly score a_t is calculated by summing the individual anomaly scores for each stream $a_t = \sum_{j=1}^k a_{j,t}$. This mapping of the vector of anomaly scores into a single value also facilitates the motion tracking functionality. If a noticeable change in a_t occurs, based on a threshold, while at least one stream is anomalous, this implies the start of an anomalous behavior. This procedure makes use of the history of the activity state inside the environment through the usage of *exponential smoothing* to monitor the a_t in order to avoid the noisy samples, hence reducing the false alarm rate. The smoothed sum B_t is calculated as follows

$$B_t = (1-\beta)B_{t-1} + \beta a_t, B_0 = a_0 \quad (6)$$

where β is the smoothing coefficient. Smoothing the values also implicitly makes use of the locality of human motion, meaning that the human will continue to affect the same stream and/or other streams near it, causing the smoothed sum of anomaly scores to have higher values during the motion period.

3) *Signal Behavior Updater*: Due to the dynamic changes in the environment, e.g. changes in temperature and humidity levels, the current state can deviate significantly from the stored normal profiles, degrading performance. Therefore, the systems needs to update the stored profiles during the online phase. The technique we employ for handling the update process continuously updates the estimated density in Equation 1 by adding $x_{j,t}$'s that do not have high anomaly scores in average to it. In particular, during the monitoring phase, the system groups the consecutive $x_{j,t}$'s in disjoint groups of size l_{update} . The group that has an average anomaly score of less than one is added to the normal profile. The parameter l_{update}

can be tuned to provide the desired performance. We quantify the effect of the l_{update} parameter in Section III-C.

Adding new data to the normal profiles implies the need to give more weight to the recent data. Thus, instead of giving equal weights to the samples used for the probability calculation in Equation 1, more weight is given to recent data. Therefore, Equation 1 is modified to:

$$\hat{f}_j(x) = \frac{1}{h_j} \sum_{i=1}^{\hat{n}} w_i V\left(\frac{x-x_{j,i}}{h_j}\right) \quad (7)$$

where $\sum_{i=1}^{\hat{n}} w_i = 1$. We choose linear weights such that $w_i = \frac{i}{\hat{n}(\hat{n}+1)/2}$ where \hat{n} is the number of sliding windows collected during the silence period and the newly added sliding windows in the online phase which were found normal (i.e. not anomalous). We found that exponential weights do not provide good performance due to the high discrimination introduced between older and newer data.

E. Motion Tracking Module

After a global detection alarm is triggered by the *Motion Detection Module*, the *Motion Tracking Module* is activated. This module is responsible for inferring the location of the moving entity. We employ a Sequential Importance Sampling with Resampling (SISR) [2], [8] particle filtering algorithm to approximate the posterior probability representing the location of the moving entity based on the anomaly scores assigned to each stream, the location of these streams, and motion model capturing the mean and variance of the human gait speed.

Formally, we want to estimate the location of a single moving entity, r_t , using the RSS vector S_t by calculating posterior

$$p(r_t|S_t) \propto p(S_t|r_t) \int p(r_t|r_{t-1})p(r_{t-1}|S_{t-1})dr_{t-1} \quad (8)$$

where the term $p(S_t|r_t)$ is the likelihood of obtaining the RSS vector S_t given the human presence at location r_t . The term $p(r_t|r_{t-1})$ represents the tracked entity's motion model and the term $p(r_{t-1}|S_{t-1})$ is posterior calculated at time step $t-1$.

We use a particle filter to estimate the posterior by representing it by a set of random weighted N particles $\{r_{i,t}, z_{i,t}\}_{i=1}^N$, where $r_{i,t}$ and $z_{i,t}$ represent the location and weight of particle i respectively at time instance t . The particle filter updates the posterior according to the following three steps which are iteratively applied after obtaining each new RSS vector S_t :

1) *Importance Sampling*: First, we perform the prediction step in which the next location of each particle $r_{i,t}$ is sampled from the $p(r_t|r_{t-1})$ distribution based on its current location $r_{i,t}$. This distribution represents the adopted motion model of the tracked entity. We use a model that captures walking patterns for humans, where the user speed, in meter/second, follows a normally distributed variable $\mathcal{N}(1.5m/s, 0.0144m^2/s^2)$ [3]. We also use the change of the stream that has the highest anomaly score to determine the direction of motion. In particular, for each particle $r_{i,t}$, we first determine the direction of the motion then the distance. To determine the direction of the motion, if the most anomalous

stream changes from one time step to the next, then the direction of motion is the vector starting from the center of old stream stream to the center of the new stream. On the other hand, if the most anomalous stream does not change remains between time steps, then the direction is sampled from a uniform distribution. Finally, a random sample is drawn from the motion model distribution to determine the distance.

The update step is then performed to assign importance weights to each particle based on the distribution $p(S_t|r_{i,t})$ which is the likelihood of obtaining the RSS vector S_t given the human presence at location $r_{i,t}$. The importance weight is calculated based on the anomaly score of the different streams and the distance between the particle and each stream. Previous results [6], [34] showed that the maximum change in RSS occurs when the human cuts the line-of-sight (LOS) between the AP and MP and the effect decreases as we move away from this LOS. Therefore, we assign the weight of each particle relative to a certain stream based on an elliptical weighting model [34]. However, instead of using the model to determine whether the moving entity is crossing the LOS or not, we use the elliptical weighting model to determine the distance between each particle and the LOS of the stream. In particular, for stream j , given its anomaly score $a_{j,t}$ at time instant t , the weight ($z_{ij,t}$) assigned to particle i based on this stream is equal to:

$$z_{ij,t} = a_{j,t} \frac{d_j}{d_{AP_j,i} + d_{MP_j,i}} \quad (9)$$

where d_j is the length of stream j (distance between the AP and MP of this stream), $d_{AP_j,i}$ is the distance between the particle and the AP, and $d_{MP_j,i}$ is the distance between the particle and the MP. This is intuitive as when the anomaly score of the stream increases or the distance between the particle and the stream decreases, the particle weight increases.

To fuse the particle weights from the different streams, we experimented with different fusion functions that took into account either a representation of the weights from all streams or the most anomalous n streams. We found that the maximum function gives the best results. The intuition behind using the maximum function is that it avoids two extreme cases that we found empirically to occur frequently: 1) fusing weights of several streams that have only one anomalous stream resulting in an overall low weight leading to a frequent divergence of the particles and 2) fusing weights of streams that have noisy anomaly scores which results in an unrepresentative set of particles, i.e. high weights are given to particles that should have been discarded. Therefore, the weight ($z_{i,t}$) for particle i at time t based on all streams is calculated as:

$$z_{i,t} = \max_j z_{ij,t} \quad (10)$$

Finally, the weights assigned to all particles are normalized.

2) **Resampling**: To prevent the divergence of particles, particles with small weights are eliminated if their percentage of the total population exceeds a certain threshold. The effective sample size is calculated as $\hat{N}_{\text{eff}} = \frac{1}{\sum_{i=1}^N (z_{i,t})^2}$. If $\hat{N}_{\text{eff}} < N/2$, the particles are resampled by drawing N particles with replacement according to the importance weights.

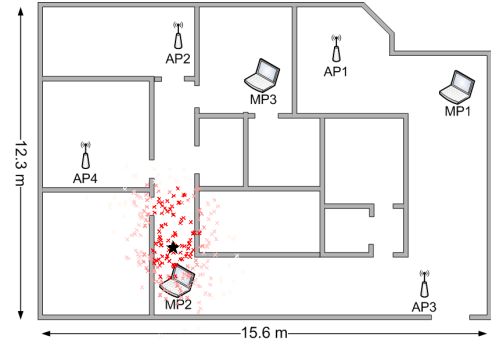


Fig. 3. An example (overlaid on Testbed 1) showing the different particle weights (darker particles have higher weights) and the estimated entity location at the centroid.

3) **Location Estimation**: The final entity location r_t is estimated as the centroid of the particles at time t as $r_t = \sum_{i=1}^N r_{i,t} z_{i,t}$ (Figure 3).

III. EXPERIMENTAL EVALUATION

In this section, we study the effect of the different parameters on the performance of *Ichnaea's* motion detection and tracking capabilities. Due to space constraints, we discuss in details the effect of different parameters on *Ichnaea* in Testbed 1 and summarize *Ichnaea's* performance in testbeds 2 and 3 in Section III-E. We leave the comparison with the state-of-the-art systems to Section IV.

A. Experimental Testbeds and Data Collection

We used three large scale testbeds, deployed in typical WLAN environments rich in multipath. The first testbed is an office apartment of approximately 186 m² (about 2000 ft²). The second testbed covers a building floor with an area of 352 m² (about 3790 ft²). The third testbed is the second floor of a two-floor home building with an area of 140 m² (about 1500 ft²). All testbeds were covered with typical furniture. For Testbed 1, we used four Cisco Aironet 1130AG series access points and three Dell laptops equipped with D-Link AirPlus G+ DWL-650+ Wireless NICs as MPs. As for Testbed 2, we used seven Cisco Aironet 1130AG series access points and two Dell laptops equipped with D-Link AirPlus G+ DWL-650+ Wireless NICs as MPs. Finally, for Testbed 3, we used four Cisco Aironet 1130AG series access points and three Dell laptops equipped with D-Link AirPlus G+ DWL-650+ Wireless NICs as MPs.

For all testbeds, the access points were operating on different channels. The experiments were conducted in typical IEEE 802.11b environments. Figures 3 and 4 show the layouts of the experiments. Because of the signal attenuation due to obstruction and the distance between some of the access points and monitoring points only 11 of the theoretically possible 12 streams in Testbed 1 and 8 of the 14 streams in Testbed 2 were sensed.

For the data collection, sets of normal (silence) state readings and motion readings were collected for each testbed. For Testbed 1, the data collected included three motion sets, each

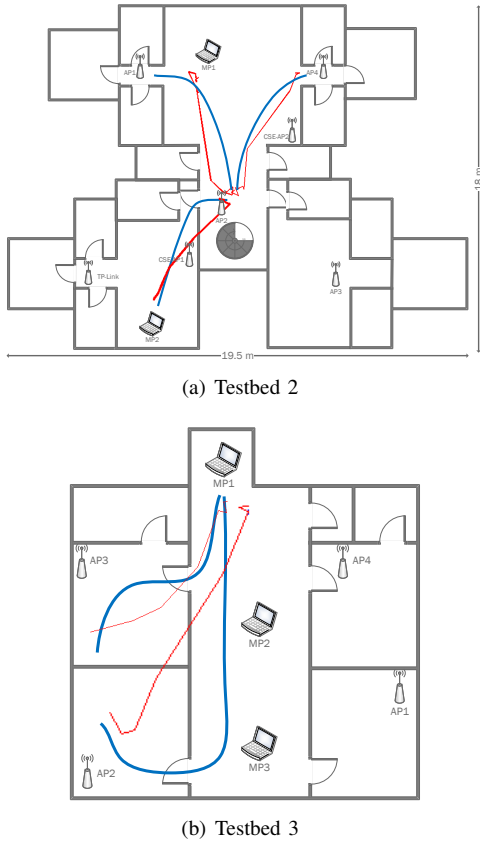


Fig. 4. Examples showing sample actual paths in blue and the corresponding estimated paths in red.

covering the entire area of the testbed. For Testbed 2 and Testbed 3, the data collected included motion sets in which the user moved from the entrance to different rooms on the floor. Samples of the motion sets are shown in blue in figures 4(a) and 4(b). To record the ground truth for the motion paths, a grid of locations was created and the moving person logged the exact time of passing each point of the grid. We used a sampling rate of one sample per second using the active scanning technique [37].

B. Evaluation Metrics

We used three metrics to analyze Ichnaea's detection performance: the false positive (FP) rate, the false negative (FN) rate and the F-measure. The false positive rate refers to the probability that the system generates an alarm while there is no human motion in the area of interest, as opposed to the true positive (TP) rate which refers to the probability that the system generates an alarm while there is human motion. The false negative rate refers to the probability that the system fails to detect the human motion in any place in the area. We also use the F-measure which refers to the harmonic mean of the precision and recall, where the precision is $\frac{TP}{TP+FP}$ and the recall is $\frac{TP}{TP+FN}$. The F-measure's importance is that it provides a single value to measure the effectiveness of the detection system [26].

For Ichnaea's tracking performance, we used the median distance error as the performance measure of the difference

	Basic Detection Procedure	Silence Profile Update	Decision Smoothing (Ichnaea Perf.)
FN Rate	0.0672	0.0876	0.0468
FP Rate	0.2158	0.1176	0.0378
F-measure	0.8683	0.8989 (3.52%)	0.9574 (10.26%)

TABLE II

ICHNAEA'S MOTION DETECTION PERFORMANCE AND ENHANCEMENT PERCENTAGE INTRODUCED BY EACH DETECTION MODULE.

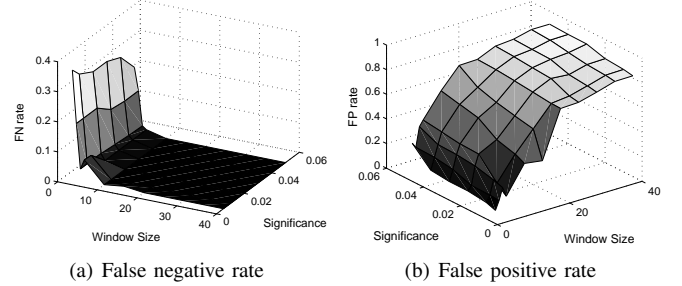


Fig. 5. Analysis of the Basic Detection Module parameters for Testbed 1.

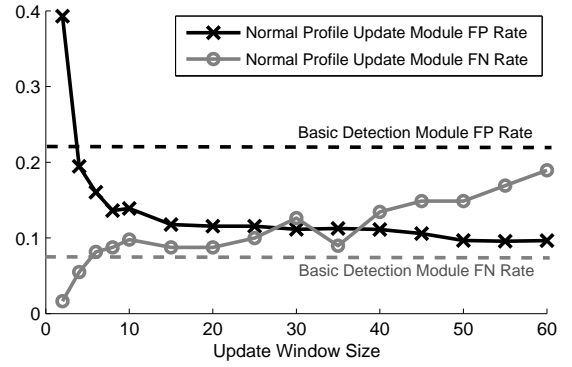


Fig. 6. Effect of the update window size parameter (l_{update}).

between Ichnaea's estimation and the actual human's position.

C. Motion Detection Module Performance

In this section, we present the effect of the different system parameters on the accuracy of Ichnaea motion detection capabilities. Table II summarizes the performance for Testbed 1.

1) *Basic anomaly detector*: This procedure requires the selection of the sliding window size l and the significance α . Figure 5 illustrates the effect of these parameters. The figure shows that choosing a too short window size will make the system less sensitive to human motion. On the other hand, choosing a very large window size will introduce a very high FP rate. For the significance parameter, as α decreases, the FP rate decreases and the FN rate slightly increases. This means that increasing the significance will result in less system sensitivity. Therefore, to balance the different performance metrics, we choose $l = 5$ and $\alpha = 0.01$.

2) *Silence profile updater*: For this module, the update window size l_{update} is required. Choosing a too small l_{update} will make the system very sensitive to noisy readings, causing a high FP rate. On the other hand, a very large l_{update} will make the system less sensitive to human motion causing a higher FN

rate. Figure 6 illustrates the effect of the update window size on the system performance when $l = 5$ and $\alpha = 0.01$. The figure shows that an update window size between 10 and 20 is sufficient to reduce the high FP rate without causing much increase to the FN Rate. Thus, we choose $l_{update} = 15$.

Although update window sizes that are more than 10 achieve better FN and FP rates, hence enhancing the F-measure, we did not find that to hold for other values of the parameters l and α . Therefore, we should be conservative about increasing the update window size.

The results are summarized in Table II. The table shows that there is about 50% reduction in the FP rate which resulted in a overall F-measure enhancement of 3.52% with respect to only detecting anomalous behavior. This enhancement can be explained by the observation that updating the silence profiles reduces the effect of the temporal variations between the environment true normal profiles and the stored normal profiles by updating them. We verified that by applying the two-sample Kolmogorov-Smirnov test to the distributions of the updated profiles and the distributions of the true normal state. The test accepted the hypothesis that those distributions came from the same underlying distribution at a significance of 0.05.

3) *Detection decision smoother*: While updating the signal profiles reduces the high FP rate by updating the stored profiles, the FP rates still need to be addressed. This procedure fuses the data from all streams by summing up the anomaly scores of different streams. To reduce the FP rate, the sum is exponentially smoothed with a smoothing coefficient of 0.04. A large increment in the smoothed sum, by more than 20% to 25% from the normal level, implies a period of human motion. Our experiments show that deviations from these parameters values do not lead to significant degradation in the results.

Table II shows that this module can lead to up to 10.2% enhancement in the F-measure with respect to the *Basic Detection Module*. It is important to note that this module also reduces the FN rate, as some of the previously undetected events are now detected because this technique makes use of the history of the state of the activity as described earlier.

D. Motion Tracking Module Performance

For tracking the entity's location, this module is affected by both the parameters used by the *Motion Detection Module* as well as its own parameters.

1) *Shared parameters with the detection module*: Figure 7 shows the effect of the significance, α , and the window size, l , on the median distance error. The tracking module has a similar behavior to the detection module behavior when these parameters change. In particular, as the values of both parameters increase, the system detection sensitivity increases and so does the accuracy of the tracking procedure.

This relation could be explained by the observation that by increasing the *Ichnaea* detection sensitivity, the anomaly scores assigned to different streams are increased. This increased sensitivity also allows streams that are slightly affected by human motion to be declared anomalous. These two factors help produce more particle weights which enhances

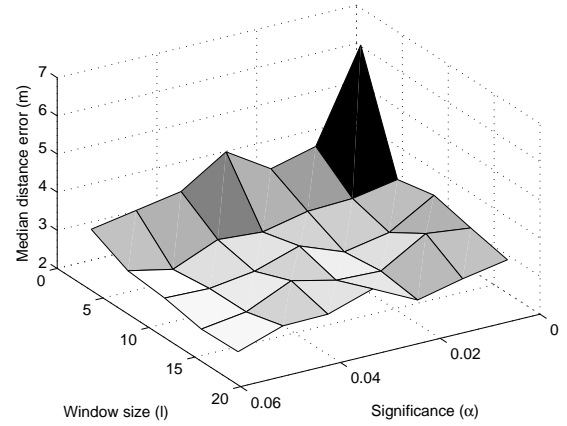


Fig. 7. Effect of window size l and significance α on the tracking accuracy in Testbed 1.

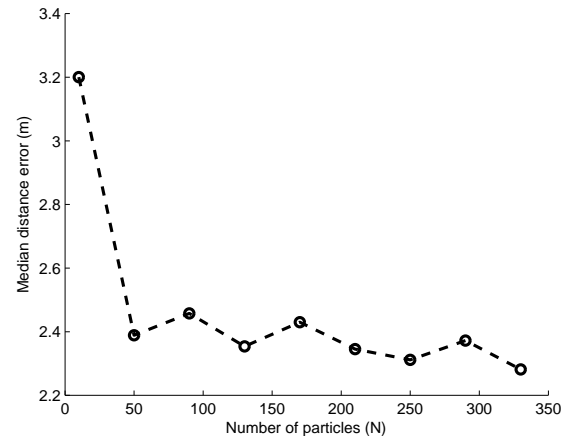


Fig. 8. Effect of number of particles on tracking accuracy in Testbed 1.

the tracking accuracy. It can be observed that the accuracy of the system settles with $\alpha = 0.04$ and $l = 10$. These values are different from the values used for the detection module. Hence, we suggest having two sets of operational parameters configurations: a motion detection parameters set and a motion tracking parameters set. *Ichnaea*'s default set is the motion detection set then, once the tracking procedure starts (i.e. human presence is detected), the system automatically switches to using the motion tracking set.

2) *Particle filter parameters*: Figure 8 shows the effect of increasing the number of particles N used by the particle filter algorithm. Intuitively, increasing the number of particles used enhances the accuracy by enhancing the representation of the estimate of the prior probability of entity's location, thus decreasing the median distance error. On the other hand, increasing the number of particles increases the processing overhead as well. We note from Figure 8 that increasing the number of particles over 150 does not incur substantial enhancement in the tracking accuracy while increasing the processing overhead significantly. Thus, we choose $N = 150$.

Finally, we examine the effect of the number of streams used to cover a testbed on the system accuracy. Figure 9 shows that as the number of streams increases, the system ability to detect human motion and in turn trigger the tracking process

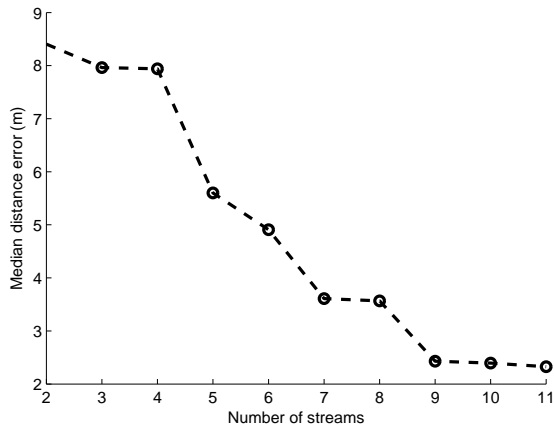


Fig. 9. Effect of number of streams on tracking accuracy in Testbed 1.

increases. It can be observed that only 9 streams achieve the best attainable accuracy.

E. Summary of System Performance for testbeds 2 and 3

In this section, we summarize the system performance for Testbed 2 and Testbed 3 (figures 4(a) and 4(b)). The same system parameters were used for both testbeds as those used for Testbed 1. The results are summarized in Table III. Comparing the results for all three testbeds, it can be noted that while in the first and third testbed the detection accuracy is better, the tracking accuracy is worse. This is explained by the observation that while Testbed 2 is the largest testbed, it is covered with fewer streams making the detection accuracy worse as human motion in some areas will not affect any streams.

On the other hand, once the tracking procedure starts, a consistent human miss-detection¹ is translated to the person leaving the area at its entrance. This technique affects the tracking accuracy in Testbed 2 less as its entrance is at the center of the testbed leading to minor shifts in the estimated path as opposed to Testbed 1 which has its entrance in one corner leading to sharper shifts in the estimated path when miss-detections occurs.

In summary, our experiments show that *Ichnaea* exhibits similar performance in all three testbeds while requiring no changes in system parameters. Moreover, only two minutes of training were used in all testbeds, which highlights *Ichnaea* ease of deployment and high accuracy.

IV. COMPARISON WITH OTHER WLAN DFP SYSTEMS

In this section, we compare *Ichnaea* to the state-of-the-art WLAN *DfP* systems, both for detection [19], [36] and tracking systems [28]. We leave the comparison with other classes of DFP systems to Section V.

A. Comparison with DfP Detection Systems

We start by a brief description of the techniques, followed by the different aspects we evaluate the techniques on. Finally, we present the results of the comparison.

¹Note that spurious and temporary mis-detections are handled by the particle filter motion model.

Results with static profiles				
	Moving Average [36]	Moving Variance [36]	MLE [19]	<i>Ichnaea</i>
FN Rate	0.1446	0.1426	0.0363	0.0468
FP Rate	0.1385	0.104	0.1547	0.0378
F-measure	0.858	0.8743	0.9099	0.9574
Results with testing profiles separated two weeks from the training profiles.				
	Moving Average [36]	Moving Variance [36]	MLE [19]	<i>Ichnaea</i>
FN Rate	0.2165	0.319	0.1653	0.0472
FP Rate	0.0711	0.1561	0.952	0.0782
F-measure	0.8449	0.7414	0.5991	0.9383
Overhead	No overhead	Minimal	Worst	Minimal

TABLE IV
PERFORMANCE COMPARISON WITH PREVIOUS *DfP* DETECTION TECHNIQUES ON TESTBED 1.

1) *Detection systems compared to Ichnaea*: Three techniques are considered for the comparison:

- 1) *The moving average technique* [36] uses a *central tendency feature*, i.e. the average. It uses two sliding window averages: a short window average representing the current system condition and a long window average representing history. The idea is to compare the two averages and if the difference is above a threshold, a detection is announced. It is important to note that the moving average technique does not require a training phase.
- 2) *The moving variance technique* [36] uses a *dispersion feature*, i.e. the variance. Similar to the moving average technique, it compares the variance of the current system state, based on a sliding window, to the variance of the silence period, obtained through a training phase. If the difference is above a threshold, a detection is announced.
- 3) *The maximum likelihood classification (MLE) technique* [19] constructs profiles for the silence period as well as for the motions period for different locations in the area of interest. The profiles represent the signal strength distribution for each stream at each location. Therefore, it involves significant training data. During the detection phase, the system finds the profile that has the maximum likelihood given a signal strength vector, one entry for each stream. If the estimated profile corresponds to a motion profile, an alarm is generated.

2) Comparison aspects:

- **Static accuracy**: accuracy when the system is evaluated with the same profiles it was trained on (if any). This is to test the best attainable accuracy.
- **Profiles' robustness**: that is how consistent the performance of the system is when the tested profiles are different from the trained ones, for example due to temporal changes in the environment. For this case, the testing data set is collected two weeks after the data sets used for training.
- **Overhead**: the effort needed to deploy the system.

3) *Comparison results*: Table IV shows the comparison results in two cases. In terms of the static accuracy, the results show that the F-measure of the *Ichnaea* system is better than other systems. Compared to the *Moving Average* and

	Area	Number of Streams	Detection FN-Rate	Detection FP-Rate	Detection F-measure	Best Median Distance Error
Testbed 1	186 m ²	11	0.0468	0.0378	0.9574	2.26 m
Testbed 2	352 m ²	8	0.0066	0.1341	0.8424	1.71 m
Testbed 3	140 m ²	12	0.0966	0.0372	0.9311	2.5 m

TABLE III
SYSTEM PERFORMANCE FOR TESTBEDS 1, 2 AND 3.

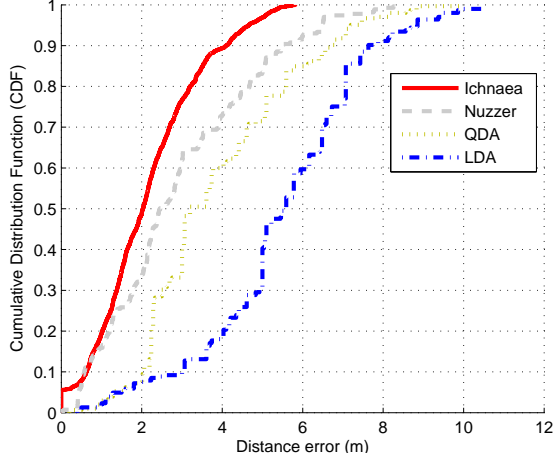


Fig. 10. CDF of distance error for Testbed 2 of *Ichnaea* compared to *Nuzzer*.

Moving Variance techniques, the *Ichnaea* system provides high accuracy due to its different modules.

In terms of profiles' robustness, the *Moving Average* technique does not store any profiles. Therefore, its overall performance is low but almost the same as the profiles change. On the other hand, the robustness of the *MLE* technique is the least as it uses the mean signal strength values as the features used for classification. Therefore, after two weeks, the distribution of the signal strength does not follow the learned one. This is why the FP rate for the *MLE* technique is too high. It can also be noted that *Ichnaea* performance is the best because *Ichnaea* uses the variance for its operation (dispersion feature) and employs techniques for adapting to changes in the environment. This is why *Ichnaea* performance is better than the *Moving Variance* in general, although the *Moving Variance* uses the same feature as *Ichnaea*.

In terms of overhead, the *Moving Average* technique has the least overhead as it does not need any learning phase. The *Moving Variance* and *Ichnaea* deployment need to construct normal profiles by collecting samples for two minutes when the human is not present. On the other hand, the *MLE* technique has the worst overhead as it constructs motion profile at each location in the area of interest in addition to the normal profile.

In summary, although the static detection accuracy of *Ichnaea* is as accurate as the *MLE* technique, the *MLE* technique has significantly higher overhead than *Ichnaea* because of its motion profile requirements. In addition, *Ichnaea* is the most robust technique to temporal changes in the training profiles and significantly outperforms the remaining techniques.

B. Comparison with DFP Tracking Systems

In this section, we compare *Ichnaea* performance to the *Nuzzer* probabilistic system presented in [28] and the Quadratic Discriminant Analysis (QDA) and Linear Discriminant Analysis (LDA) deterministic approaches presented in [35]. All are in the area fingerprinting based *DfP* tracking systems and are evaluated in Testbed 2. A fingerprint of 19 locations was built to cover the whole area of Testbed 2. A person is standing at each location about one minute to fingerprint it. The evaluation of this system was made using only 8 streams, which were observed to provide adequate accuracy for all three systems in Testbed 2. Figure 10 shows a comparison of the performance of all three systems. The figure shows that *Ichnaea* provides an enhancement in median distance error of more than 22%, 60% and 230% over *Nuzzer*, QDA and LDA respectively. It is important to note that *Ichnaea* also requires significantly less calibration overhead of only two minutes of signal recording when no one is present in the area of interest with no requirement of access to any specific areas. On the other hand, all other systems required a total calibration of 20 minutes, other than the work done to plan the grid covering the area, for a 352 m² area with the requirement of having access to all parts of the area of interest so that a person could stand there for one minute per location.

V. RELATED WORK

Device-based localization systems have been an active field of research. Several systems have been proposed for both motion detection and tracking of an entity carrying a device either with the use of special hardware like accelerometers or motion sensors [4], [16], [23], [25], or by using the existing network infrastructures like wireless networks [10], [15], [32], [37] and GSM [1], [31]. DFP systems provide an equivalent functionality without requiring any hardware which enables this new technology to be used in different applications including smart environments and intrusion detection and tracking.

Different classes of device-free localization systems have been proposed. Computer vision [14], physical contact based systems [20] and infrared-based (IR) systems [17] these technologies share the requirement of installing special hardware to handle the device-free different functionalities and are limited to line-of-sight vision or direct contact and thus they require a high cost deployment to cover large regions. Moreover, regular cameras can fail to work in the dark or in the presence of smoke, and they can cause privacy concerns. Other technologies include the usage of wireless sensors for tracking transceiver-free objects [38] as well as the usage of RFID tags [18].

Another class of device-free localization systems are radar systems. MIMO radar employs multiple transmit waveforms

	MIMO Radar-based Systems	Radio Tomographic Imaging (RTI)	Fingerprinting based WLAN Systems	<i>Ichnaea</i> System
Measured Physical Quantity	Reflection and scattering	RSS attenuation	Changes in RSS	Changes in RSS
Range (based on frequency)	Short	Long	Long	Long
Accuracy	Very High	High	High	High
Substantial Calibration Efforts	No	No	Yes	No
Robustness to changes in the environment	N/A	N/A	No	Yes
Non-LOS localization	Yes	No	Yes	Yes
Complexity of single node (or device)	High	Low	Moderate	Moderate
Number of streams	N/A (echo based)	Large (756)	Small (6)	Small (9)
Special hardware required	Yes	Yes	No	No
Covering large areas	Limited by its short range (high frequency)	Limited by number of deployed nodes (LOS)	Yes	Yes

TABLE V
COMPARISON OF DIFFERENT RF DEVICE-FREE PASSIVE TRACKING SYSTEMS.

and has the ability to jointly process the echoes observed at multiple receive antennas [5], [9]. Elements of the MIMO radar transmit independent waveforms resulting in an omnidirectional beampattern. It can also create diverse beampatterns by controlling correlations among transmitted waveforms. In MIMO, different waveforms are utilized and can be chosen to enhance performance in a number of ways. Although this class of radar systems can provide accurate detection and tracking they require complex deployments.

Radio tomographic imaging (RTI) [21], [22], [34] is another popular device-free localization technology. RTI relies on the deployment sensors and the analyzes the effect of the moving entity on each of wireless link in order to infer the intruder's location. The method takes advantage of the motion-induced variance of RSS measurements made in a wireless peer-to-peer network. Accurate detection and tracking capabilities of RTI systems require the dense deployment of a large number of wireless sensors.

WLAN device-free passive systems try to avoid the above drawbacks by using the already available wireless infrastructure. Techniques for *DfP* detection [11], [19], [36] and tracking [13], [28], [36] were introduced. The proposed techniques for the detection capability are either based on time-series analysis like the moving average and moving variance techniques proposed in [36] or based on classification using the maximum likelihood estimation [19]. As for tracking, fingerprinting based *DfP* systems [28], [29], [35] track human motion by relying on passive radio maps. Passive radio maps are constructed in the offline phase making a person stand at a number of locations covering the area of interest and recording the effect the person has on RSS readings at monitoring points. Each new reading in the online phase is classified to one of the locations in the radio map.

The *Ichnaea* system is a WLAN device-free localization system that provides both detection and single entity tracking capabilities. Compared to the previously proposed WLAN *DfP* detection techniques, the usage of the statistical anomaly detection technique, along with the other techniques devised for adapting to environment changes and refining the decision, enable *Ichnaea* to achieve low deployment overhead, high accuracy and high robustness to changes in the environment as compared to other WLAN systems that require regular professional calibration to maintain accuracy. Compared to earlier WLAN *DfP* tracking systems, *Ichnaea* requires significantly

lower overhead as it doesn't require a passive radio map and relies on tracking anomalous behavior of different wireless links to estimate the moving entity's location. Although its approach might seem similar to RTI systems, *Ichnaea* relies on a significantly smaller infrastructure and relies on detecting anomalous behavior of RSS values as compared to signal attenuation in RTI. Table V compares *Ichnaea* with the state of the art *DfP* tracking systems.

VI. CONCLUSIONS AND FUTURE WORK

We presented the *Ichnaea* system that enables device-free passive motion detection and tracking using the already installed wireless networks. *Ichnaea* uses statistical anomaly detection techniques to provide its detection capability. It also employs profile update techniques to capture changes in the environment and to enhance the detection accuracy. Once detected, we showed how *Ichnaea* uses a particle filter model based on the anomaly scores of the different streams and a human motion model for tracking the motion of a single entity in the area of interest.

We evaluated the system in three different environments, rich in multipath. The results showed that *Ichnaea* can provide an accurate detection reaching an F-measure of at least 0.93. In addition, it can track a human with a median distance error of a maximum of 2.5m. The performance of the *Ichnaea* system was compared to the previously introduced techniques for WLAN *DfP* detection and tracking systems. The results showed that *Ichnaea* outperformed the state-of-the-art techniques in terms of robustness and accuracy while maintaining minimal deployment overhead.

Currently, we are expanding *Ichnaea* in several directions including extending the approach for multiple entities tracking. Furthermore, we are performing a study of possible sources of noise in typical wireless environments, e.g. other devices inside or outside the area of interest, and how to reduce their effect. We are also studying how the detected entity's characteristics, e.g. size, shape and motion pattern, can affect the system performance. Moreover, the site configuration, i.e. the positions of the APs and MPs, can also be studied in order to optimize the system performance on different testbeds.

REFERENCES

- [1] I. Anderson and H. Muller, "Context Awareness via GSM Signal Strength Fluctuation," in *Pervasive 2006*.

- [2] M. Arulampalam, S. Maskell, N. Gordon, and T. Clapp, "A tutorial on particle filters for online nonlinear/non-gaussian bayesian tracking," *Signal Processing, IEEE Transactions on*, vol. 50, no. 2, pp. 174–188, feb 2002.
- [3] B. Auvinet *et al.*, "Reference data for normal subjects obtained with an accelerometer device," *Gait & posture*, vol. 16, no. 2, pp. 124–134, 2002.
- [4] L. Bao and S. S. Intille, "Activity Recognition from User-annotated Acceleration Data," in *Pervasive Computing (LNCS)*, vol. 3001, 2004.
- [5] I. Bekkerman and J. Tabrikian, "Target detection and localization using mimo radars and sonars," *Signal Processing, IEEE Transactions on*, vol. 54, no. 10, pp. 3873–3883, 2006.
- [6] K. El-Kafrawy, M. Youssef, and A. El-Keyi, "Impact of the human motion on the variance of the received signal strength of wireless links," in *PIMRC*, 2011, pp. 1208–1212.
- [7] P. Enge and P. Misra, "Special Issue on Global Positioning System," in *Proceedings of the IEEE*, January 1999, pp. 3–172.
- [8] N. Gordon, D. Salmond, and A. Smith, "Novel approach to nonlinear/non-gaussian bayesian state estimation," in *IEE Proc. F Radar and Signal Processing*, vol. 140, no. 2. IET, 1993, pp. 107–113.
- [9] A. Haimovich, R. Blum, and L. Cimini, "Mimo radar with widely separated antennas," *Signal Processing Magazine, IEEE*, vol. 25, no. 1, pp. 116–129, 2008.
- [10] K. Kleisouris *et al.*, "Detecting Intra-room Mobility with Signal Strength Descriptors," in *MobiHoc'10*.
- [11] A. E. Kosba, A. M. Saeed, and M. A. Youssef, "Robust WLAN Device-free Passive Motion Detection," in *WCNC'12*.
- [12] A. Kosba, A. Saeed, and M. Youssef, "RASID: A Robust WLAN Device-free Passive Motion Detection System," in *Percom'12*. IEEE, 2012, pp. 180–189.
- [13] A. E. Kosba, A. Abdelkader, and M. Youssef, "Analysis of a Device-free Passive Tracking System in Typical Wireless Environments," in *The 3rd International Conference on New Technologies, Mobility and Security*, 2009, pp. 291–295.
- [14] J. Krumm *et al.*, "Multi-Camera Multi-Person Tracking for EasyLiving," in *The Third IEEE International Workshop on Visual Surveillance*, 2000, pp. 3–10.
- [15] J. Krumm and E. Horvitz, "LOCADIO: Inferring Motion and Location from Wi-Fi Signal Strengths," 2004, pp. 4–13.
- [16] J. Krumm, L. Williams, and G. Smith, "SmartMoveX on a Graph - An Inexpensive Active Badge Tracker," in *UbiComp '02*.
- [17] M. Moghavvemi and L. C. Seng, "Pyroelectric infrared sensor for intruder detection," in *TENCON 2004. 2004 IEEE Region 10 Conference*, vol. 500. IEEE, 2004, pp. 656–659.
- [18] R. S. Moore *et al.*, "A Geometric Approach to Device-Free Motion Localization Using Signal Strength," Rutgers University, Tech. Rep. DCS-TR-674, September 2010.
- [19] M. Moussa and M. Youssef, "Smart Devices for Smart Environments: Device-free Passive Detection in Real Environments," in *IEEE PerCom Workshops*, 2009.
- [20] R. J. Orr and G. D. Abowd, "The Smart Floor: A Mechanism for Natural User Identification and Tracking," in *The ACM CHI Conference on Human Factors in Computing Systems*, vol. 2, 2000.
- [21] N. Patwari and J. Wilson, "Rf sensor networks for device-free localization: measurements, models, and algorithms," *Proceedings of the IEEE*, vol. 98, no. 11, pp. 1961–1973, 2010.
- [22] —, "Spatial models for human motion-induced signal strength variance on static links," *Information Forensics and Security, IEEE Transactions on*, vol. 6, no. 3, pp. 791–802, 2011.
- [23] M. Philipose *et al.*, "Inferring Activities from Interactions with Objects," *IEEE Pervasive Computing*, vol. 3, October 2004.
- [24] N. B. Priyantha, A. Chakraborty, and H. Balakrishnan, "The Cricket Location-Support System," in *The 6th Annual International Conference on Mobile Computing and Networking*, New York, NY, USA, 2000, pp. 32–43.
- [25] C. Randell and H. Muller, "Context Awareness by Analyzing Accelerometer Data," in *ISWC'00*, 2000, pp. 175–176.
- [26] C. J. V. Rijsbergen, *Information Retrieval*, 2nd ed. Newton, MA, USA: Butterworth-Heinemann, 1979.
- [27] D. W. Scott, *Multivariate Density Estimation: Theory, Practice, and Visualization*. Wiley, 1992.
- [28] M. Seifeldin *et al.*, "Nuzzer: A large-scale device-free passive localization system for wireless environments," *Mobile Computing, IEEE Transactions on*, vol. 12, no. 7, pp. 1321–1334, 2013.
- [29] M. A. Seifeldin, A. F. El-keyi, and M. A. Youssef, "Kalman filter-based tracking of a device-free passive entity in wireless environments," in *WiNTECH'11*. New York, NY, USA: ACM, 2011, pp. 43–50.
- [30] B. W. Silverman, *Density Estimation for Statistics and Data Analysis*. Chapman & Hall/CRC, April 1986.
- [31] T. Sohn *et al.*, "Mobility Detection Using Everyday GSM Traces," in *UbiComp '06*.
- [32] M. Wallbaum and S. Diepolder, "A Motion Detection Scheme For Wireless LAN Stations," in *The 3rd International Conference on Mobile Computing and Ubiquitous Networking*, 2006.
- [33] R. Want *et al.*, "The Active Badge Location System." *ACM Trans. Inf. Syst.*, vol. 10, no. 1, 1992.
- [34] J. Wilson and N. Patwari, "Radio tomographic imaging with wireless networks," *Mobile Computing, IEEE Transactions on*, vol. 9, no. 5, pp. 621–632, 2010.
- [35] C. Xu *et al.*, "Improving rf-based device-free passive localization in cluttered indoor environments through probabilistic classification methods," in *The 11th international conference on Information Processing in Sensor Networks*. ACM, 2012, pp. 209–220.
- [36] M. Youssef, M. Mah, and A. Agrawala, "Challenges: Device-free Passive Localization for Wireless Environments," in *The 13th Annual ACM International Conference on Mobile Computing and Networking*. ACM, 2007, pp. 222–229.
- [37] M. A. Youssef and A. Agrawala, "The Horus WLAN Location Determination System," in *Communication Networks and Distributed Systems Modeling and Simulation Conference*, 2005, pp. 205–218.
- [38] D. Zhang *et al.*, "An RF-Based System for Tracking Transceiver-Free Objects," in *PerCom '07*.



Ahmed Saeed received his B.Sc. in Computer Science from Alexandria University, Egypt in 2010. He is currently a research assistant in the Department of Computer Science and Engineering at the Egypt-Japan University of Science and Technology (E-JUST), Egypt. His research interests include context awareness, systems research and networking protocol design. He is a student member of IEEE.



Ahmed Kosba received his B.Sc. and M.Sc. in Computer Science from Alexandria University, Egypt in 2009 and 2012 respectively. He is currently a Ph.D. Student in the Department of Computer Science, University of Maryland at College Park. His research interests include location determination systems, pattern recognition and security. He is a student member of IEEE.



Moustafa Youssef is an Associate Professor at Alexandria University and Egypt-Japan University of Science and Technology (E-JUST), Egypt. He received his Ph.D. degree in computer science from University of Maryland, USA in 2004 and a B.Sc. and M.Sc. in computer science from Alexandria University, Egypt in 1997 and 1999 respectively. His research interests include mobile wireless networks, mobile computing, location determination technologies, pervasive computing, and network security. He has eight issued and pending patents. He is an

area editor of the ACM MC2R and served on the organizing and technical committees of numerous conferences. Dr. Youssef is the recipient of the 2003 University of Maryland Invention of the Year award, the 2010 TWAS-AAS-Microsoft Award for Young Scientists, the 2012 Egyptian State Award, among others.